www.czasopisma.pan.pl PAN POLSKA AKADEMIA NAUK www.journals.pan.pl

PAN ARCHIVES OF ACOUSTICS
Vol. **43**, No. 4, pp. 669–679 (2018)

DOI: 10.24425/aoa.2018.125160

Analytical Model of Three-Dimensional Ultrasonic Beam Interaction with an Immersed Plate

Hanane SOUCRATI[(1)], Ahmed CHITNALAH[(1)], Noureddine AOUZALE[(1)], Hicham JAKJOUD[(2)]

[(1)] *Electrical Systems and Telecommunications Laboratory*
Cadi Ayyad University
BP 549, Av. Abdelkarim Elkhattabi, Guéliz Marrakesh, Morocco; e-mail: hanane.soucrati@edu.uca.ma

[(2)] *Energy Engineering Materials and Systems Laboratory*
Ibn Zohr University
BP 1136, Agadir, Morocco

(*received December 25, 2017; accepted June 28, 2018*)

This paper proposes an analytical model to describe the interaction of a bounded ultrasonic beam with an immersed plate. This model, based on the Gaussian beams decomposition, takes into account multiple reflections into the plate. It allows predicting three-dimensional spatial distributions of both transmitted and reflected fields. Thereby, it makes it easy to calculate the average pressure over the receiver's area taking into account diffraction losses. So the acoustical parameters of the plate can be determined more accurately. A Green's function for the interaction of an ultrasonic beam with the plate is derived. The obtained results are compared to those given by the angular spectrum approach. A good agreement is seen showing the validity of the proposed model.

Keywords: ultrasonic modeling; immersed plate; Gaussian beams decomposition; Green's functions; NDUT.

1. Introduction

The Non-Destructive Testing (NDT) is a group of techniques widely used in science and industry to evaluate the changes in the properties of a material, a component or a system. The aim of all NDT methods is monitoring the investigated object without causing damage, change of properties or impairment of performance in future use (Cartz, 1995; Van Hemelrijck, Anastassopoulos, 1996). The Non-Destructive Ultrasonic Testing (NDUT) is one of the most commonly used techniques and its application has been increasing rapidly over the last few decades since the electronic equipment has become cheaper and more readily available (Perdijon, 1993; Blitz, Simpson, 1996; Schmerr, Lester, 2013; Langenberg *et al.*, 2012). This technique consists of propagating a low amplitude waves through a material to measure the time of flight and any change of intensity for a given distance. It consequently allows determining the velocity and the absorption coefficient leading to deduce material properties (Gunarathne, Christidis, 2002; Aouzale *et al.*, 2010; Hull *et al.*, 1996; Shankar, 2001).

One of the situations encountered is ultrasonic inspection of a plate immersed in water (Deschamps, Hosten, 1992; Lowe, 1995; Moilanen *et al.*, 2006; Glauser *et al.*, 2001). Characterization of immersed thick plate is easier than the case of thin plate, especially when an ultrasonic spectroscopy technique is used (Kline, 1984). Kinra and Dayal (1988) developed a technique for inspection of a thin immersed plate. They used ultrasonic transmission coefficient to determinate the elastic constant of materials. This technique is useful for thin as well as thick plate and also for either dispersive or nondispersive media. In other work, Kinra and Iyer (1995) calculate one of the four properties of an immersed thin plate (longitudinal wave velocity, attenuation, thickness or density) assuming that the three others are known. Unlike Kinra and Iyer's technique, El Mouhtadi *et al.* (2012) propose a method for simultaneous determination of all of these properties by performing a least squares fit between theoretical and experimental data points.

The NDUT is also used for monitoring defect in the plate by locating and sizing accurately even the

smallest ones. It is based on the detection of anomalies, such as discontinuities in materials by analyzing the phenomena of reflection and transmission of ultrasonic waves propagating through the immersed plate (Lee, Staszewski, 2003a; 2003b; 2007a; 2007b; Leiderman *et al.*, 2005; Soucrati *et al.*, 2013).

In the theoretical study of reflection phenomena, the plane wave theory is often used (Carcione, 1996). However, it is well known that this simple model does not provide an accurate description of the situations encountered experimentally especially when there are standing waves resulting from the multiple reflections inside the plate (Rose, 1999). Besides, diffraction affects the accuracy of the measurement, in particular when the plate is located beyond the near field zone (Seki *et al.*, 1956).

Conversely, to overcome these restraints, the Gaussian beam decomposition method is investigated. It is based on the modeling of the wave field by a set of Gaussian beams. Each beam is propagated independently. The total wave field at the receiver is constituted by a superposition of all Gaussian beams arriving in the receiver vicinity. The advantage of the resulting computational algorithm consists in its independence of studied geometric structure and of observation point position.

The Gaussian beam decomposition method is proposed for the first time by Popov *et al.* (1980) to describe the wave fields in two-dimensional point source problem. Basing on the work of Babich and Pankratova (1973), which is founded on a mathematical investigation of the Green's function, Popov (1982a; 1982b) develops the Gaussian beam decomposition method to compute the wave fields in three-dimensions. The first attempts of numerical applications of this method to wave field modeling are presented by Kachalov and Popov (1981) and Cerveny *et al.* (1982). In literature, this method is applicable to acoustic, electromagnetic and elastic wave fields modeling.

In this work, an analytical model to predict a three-dimensional ultrasonic beam is derived. This model gives both reflected and transmitted fields, as well as the field inside the plate. The incident field generated by a circular transducer is expressed using the decomposition in a set of Gaussian beams. The reflected and the transmitted pressure fields at each side of the plate are expressed using the method given by Makin *et al.* (2000). The main contribution of the proposed model lies in taking into account multiple reflections of the ultrasonic wave inside the plate as well as diffraction effect. The model allows also choosing the position of the plate without restraint.

Comparison between the results obtained by the derived model and those given by the Angular Spectrum Approach (ASA) method shows a good agreement which proves the validity of the derived model.

In the rest of this paper, the theory background is presented in the second section; explanation of the problem configuration and a brief presentation of the two theories, the ASA and the Green's function. The third section is dedicated to the derived model; expressions of the ultrasonic field in three-dimension are given. The fourth section provides simulation results, validation of the model and the plate characterization. Conclusions are made in the last section.

2. Theory background

2.1. Studied configuration

We consider the geometric situation of Fig. 1. A transmitting transducer in the form of a piezoelectric disc of radius a, positioned at the plan $z = 0$, radiates an ultrasonic beam at frequency f_0 in water. The plate to be analyzed is of a thickness d, positioned at the focal point $z = z_f$ on the axis of propagation (focal point = (transmitter radius)^2/medium wavelength). It is assumed that the beam falls on the plate with a normal incidence. The interfaces of the plate are in the planes $z = z_1$ and $z = z_2$. The signal transmitted through the plate, is received by a second transducer of radius b located at the $z = 2z_f$ position. However, the reflected wave is received by the emitting transducer itself.

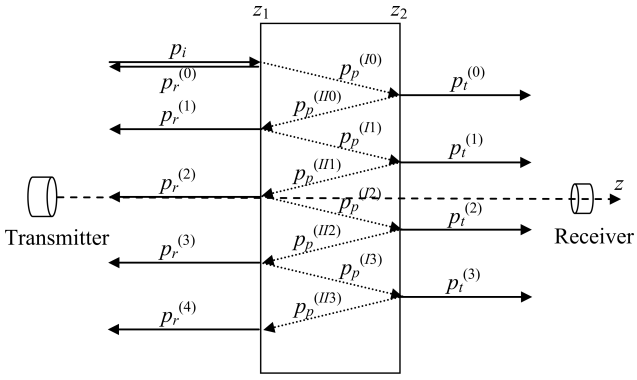

Fig. 1. Geometrical configuration.

The fluid surrounding the plate is water which is characterized by its acoustic parameters; the density ρ_0, the velocity c_0, the acoustic impedance Z_0, the wave number k_0 and the attenuation coefficient α_0.

The plate is characterized by its acoustic parameters; the density ρ_1, the longitudinal sound speed c_1, the acoustic impedance Z_1, the wave number k_1 and the attenuation coefficient α_1.

2.2. Propagation equation

The ultrasound propagation in a homogeneous medium is modeled by the wave equation which can be written as (Westervelt, 1963):

$$\frac{\partial^2 p}{\partial z^2} + \Delta_\perp p - \frac{1}{c^2}\frac{\partial^2 p}{\partial t^2} + \frac{2\alpha}{c\omega^2}\frac{\partial^3 p}{\partial t^3} = 0, \tag{1}$$

where p is the acoustic pressure, $\Delta_\perp = \frac{1}{r}\frac{\partial}{\partial r}\left(r\frac{\partial}{\partial r}\right) + \frac{1}{r^2}\frac{\partial^2}{\partial \theta^2}$ is the transverse Laplacian in polar coordinates (r, θ), z is the coordinate on the propagation axis, ω is the pulsation, c is the velocity and α is the coefficient of absorption.

In the case of a harmonic excitation, the wave equation can be written as (Rossi, 1986):

$$\frac{\partial^2 p}{\partial z^2} + \Delta_\perp p + k^2 p = 0, \tag{2}$$

where $k = \frac{\omega}{c}\sqrt{1 + i2\alpha\frac{c}{\omega}} \approx k_0 + i\alpha$, i is the unit imaginary number ($i^2 = -1$) and $k_0 = \omega/c$ is the wave number.

In the rest of the paper, the index s refers to the angular spectrum approach (ASA), while the index g is used for Gaussian beam decomposition (GBD).

2.3. Angular spectrum approach

The angular spectrum approach (ASA) is a mathematical tool that allows differential equations resolution. This approach permits the ultrasonic propagation simulation between two parallel planar surfaces. Its goal is to calculate the resulting field in a plane parallel to a known field (Williams, Maynard, 1982; Orofino, Pedersen, 1993a; 1993b; Wu *et al.*, 1996a; 1996b; 1997; Du *et al.*, 2009; 2013). It is based on applying the two-dimensional spatial Fourier transform to the wave equation (Goodman, 1968).

$$P(k_r, z) = \frac{1}{2\pi}\int_0^{2\pi}\int_0^{+\infty} p(r, z)\, \mathrm{e}^{-ik_r r\cos\theta} r\, \mathrm{d}r\, \mathrm{d}\theta, \tag{3}$$

thus

$$P(k_r, z) = \int_0^{+\infty} p(r, z) J_0(k_r r) r\, \mathrm{d}r, \tag{4}$$

where P is the two-dimensional spatial Fourier transform of p, k_r is the wave number along r direction and $J_0(x)$ is the 0-th order Bessel function of the first kind, $p(r, z)$ is $p(r, \theta, z)$; θ is omitted since an axisymmetric circular source is used, then p is independent of θ.

Applying the two-dimensional spatial Fourier transform to Eq. (2) yields

$$\frac{\partial^2 P}{\partial z^2} + (k^2 - k_r^2)P = 0. \tag{5}$$

The solution of this differential equation can be put in the form

$$P(k_r, z) = P(k_r, 0)\, \mathrm{e}^{-iz\sqrt{k^2 - k_r^2}}. \tag{6}$$

Since there is a uniform excitation of an axisymmetric circular source of radius a, then

$$P(k_r, 0) = ap_0 \frac{J_1(ak_r)}{k_r}, \tag{7}$$

where $J_1(x)$ is the first order Bessel function of the first kind and p_0 is the pressure level at the source given in [Pa].

Finally, the pressure field $p(r, z)$ is the spatial inverse Fourier transform (Hankel transform) of Eq. (6)

$$p(r, z) = \int_0^{+\infty} P(k_r, 0) J_0(rk_r)\, \mathrm{e}^{-iz\sqrt{k^2 - k_r^2}} k_r\, \mathrm{d}k_r. \tag{8}$$

By developing Eq. (8), the pressure field can be expressed in the following manner

$$p(r, z) = ap_0 \int_0^{+\infty} J_0(rk_r) J_1(ak_r)\, \mathrm{e}^{-iz\sqrt{k^2 - k_r^2}}\, \mathrm{d}k_r. \tag{9}$$

The incident field in water is then written as

$$p_{is}(r, z) = ap_0 \int_0^{+\infty} J_0(rk_r) J_1(ak_r)\, \mathrm{e}^{-iz\sqrt{k_0^2 - k_r^2}}\, \mathrm{d}k_r. \tag{10}$$

The reflection coefficient of the plate in the same configuration as in Fig. 1 is (Rossi, 1986)

$$R_p(k_r) = r_1 + t_1 t_2 r_2 \frac{\mathrm{e}^{-i2d\sqrt{k_1^2 - k_r^2}}}{1 - r_2^2 \mathrm{e}^{-2id\sqrt{k_1^2 - k_r^2}}}, \tag{11}$$

where $r_1 = \frac{Z_1 - Z_0}{Z_0 + Z_1}$ and $r_2 = \frac{Z_0 - Z_1}{Z_0 + Z_1}$ are the reflection coefficients of the interface water-plate-water in the case of normal incidence. And, $t_1 = \frac{2Z_1}{Z_0 + Z_1}$ and $t_2 = \frac{2Z_0}{Z_0 + Z_1}$ are the transmission coefficients.

In the same manner as in (Rossi, 1986), the transmission coefficient of the plate is

$$T_p(k_r) = t_1 t_2 \frac{\mathrm{e}^{-id\sqrt{k_1^2 - k_r^2}}}{1 - r_2^2 \mathrm{e}^{-2id\sqrt{k_1^2 - k_r^2}}}. \tag{12}$$

Then, using Eq. (11), the reflected field is

$$p_{rs}(r, z) = ap_0 \int_0^{+\infty} R_p(k_r) J_0(rk_r) \cdot J_1(ak_r)\, \mathrm{e}^{-i(2z_1 - z)\sqrt{k_0^2 - k_r^2}}\, \mathrm{d}k_r. \tag{13}$$

Similarly, using Eq. (12), the transmitted field is

$$p_{ts}(r, z) = ap_0 \int_0^{+\infty} T_p(k_r) J_0(rk_r) \cdot J_1(ak_r)\, \mathrm{e}^{-i(z - d)\sqrt{k_0^2 - k_r^2}}\, \mathrm{d}k_r. \tag{14}$$

Inside the plate, the field is expressed as

$$p_{ps}(r, z) = ap_0 \int_0^{+\infty} P_l(k_r, z) J_0(rk_r) J_1(ak_r)\, \mathrm{d}k_r \tag{15}$$

with

$$P_l(k_r, z) = t_1 \frac{\mathrm{e}^{-i(z-z_1)a^* - iz_1 b^*} + r_2\,\mathrm{e}^{-i(2d-z+z_1)a^* - iz_1 b^*}}{1 - r_2^2 \mathrm{e}^{-2ida^*}}, \tag{16}$$

where

$$a^* = \sqrt{k_1^2 - k_r^2}, \qquad b^* = \sqrt{k_0^2 - k_r^2}.$$

2.4. Green's function method

Using Green's functions (Green, 1852), the solution of wave Eq. (2) can be written in the following form

$$p(r, z) = \iint p(r', 0) G(r, z|r', 0)\,\mathrm{d}s, \tag{17}$$

where $p(r', 0)$ is a source element at $r = r'$ and $z = z' = 0$.

The Green's function $G(r, z|r', z')$ is defined by (Ingard, Morse, 1968)

$$G(r, z|r', z') = \frac{ik}{4\pi D}\mathrm{e}^{-ikD}. \tag{18}$$

In the case of the axisymmetric source, D, the distance between the source point $(r',\ z')$ and the measurement point $(r,\ z)$, is expressed as

$$D = \sqrt{r^2 + r'^2 - 2rr'\cos(\theta') + (z - z')^2}, \tag{19}$$

where θ' is the angel between the radius vector $\mathbf{r}'$ to the source point and the radius vector $\mathbf{r}$ to the measurement point.

By introducing the binomial expansion of the square root, the distance D can be developed as

$$D = (z - z') + \frac{r^2 + r'^2 - 2rr'\cos(\theta')}{2(z - z')} + \frac{\left[r^2 + r'^2 - 2rr'\cos(\theta')\right]^2}{8(z - z')^3} + \ldots \tag{20}$$

Applying the Fresnel approximation (Goodman, 1968)

$$D \approx \frac{r^2 + r'^2}{2(z - z')} - \frac{rr'\cos(\theta')}{z - z'} + (z - z'). \tag{21}$$

In general, for the D appearing at the denominator of Eq. (18), the error introduced by eliminating all the terms except $(z - z')$ is small enough. So, $D \approx z - z'$.

However, the error is greatly more significant for the D appearing in the exponential. This is due to the fact that the distance D is multiplied by a very large number k. In addition, a small change in the phase can change the exponential value significantly. That is why first and second terms of the binomial approximation of Eq. (20) are retained in the exponent. So Eq. (18) becomes

$$G(r, z|r', z') = \frac{ik}{4\pi(z - z')} \cdot \mathrm{e}^{-ik\frac{r^2 + r'^2}{2(z - z')}}\,\mathrm{e}^{ik\frac{rr'}{z - z'}\cos(\theta')}\,\mathrm{e}^{-ik(z - z')}. \tag{22}$$

Integrating over θ', the pressure field is expressed as

$$p(r, z) = \frac{ik}{2}\int_0^{+\infty} p(r', 0) J_0\left(k\frac{rr'}{z}\right) \cdot \frac{\mathrm{e}^{-ikz}}{z}\mathrm{e}^{-ik\frac{r^2 + r'^2}{2z}} r'\,\mathrm{d}r'. \tag{23}$$

Putting

$$g(r, z|r', z') = \frac{ik}{2}\frac{\mathrm{e}^{-ik(z - z')}}{(z - z')} J_0\left(k\frac{rr'}{z - z'}\right)\mathrm{e}^{-ik\frac{r^2 + r'^2}{2(z - z')}}. \tag{24}$$

Therefore, the field can be written as (Hamilton, Blackstock, 1998)

$$p(r, z) = \int_0^{+\infty} p(r', 0) g(r, z|r', 0)\, r'\,\mathrm{d}r'. \tag{25}$$

We choose to note g_0 for water and g_p for the plate.

3. Derived model

3.1. Incident field

By developing the source term $p(r', 0)$ in Gaussian Beams Decomposition (Wen, Breazeale, 1988), one can obtain

$$p(r', 0) = p_0 \sum_{n=1}^{N} A_n\,\mathrm{e}^{-B_n\left(\frac{r'}{a}\right)^2}, \tag{26}$$

where A_n and B_n are Gaussian coefficients that depend on the source shape (Jakjoud *et al.*, 2014).

The incident field can be written as

$$p_{ig}(r, z) = \int_0^{+\infty} p(r', 0) g_0(r, z|r', 0)\, r'\,\mathrm{d}r'. \tag{27}$$

Replacing the source term in Eq. (27), and using the first exponential Weber integral (Korenev, 2002), the incident field in water is

$$p_{ig}(r, z) = p_0\,\mathrm{e}^{-ik_{p0}z}\sum_{n=1}^{N}\frac{A_n}{f_{in}(z)}\,\mathrm{e}^{\frac{-B_n}{f_{in}(z)}\left(\frac{r}{a}\right)^2} \tag{28}$$

with

$$f_{in}(z) = 1 - i\frac{z}{z_n} \tag{29}$$

and

$$z_n = \frac{k_0 a^2}{2B_n}; \qquad k_{p0} = k_0 - i\alpha_0. \tag{30}$$

3.2. Reflected field

The idea is to decompose the total reflected field into a series of reflections

$$p_{rg}(r,z) = p_r^{(0)} + p_r^{(1)} + p_r^{(2)} + \ldots \tag{31}$$

The reflected field at the interface water-plate can be expressed as (Makin *et al.*, 2000)

$$p_r^{(0)}(r,z) = \int_0^{+\infty} r_1 p_{ig}(r',z_1) g_0(r,z|r',z_1) r'\,\mathrm{d}r'. \tag{32}$$

Replacing the expression of $p_{ig}(r',z_1)$ from Eq. (28) in Eq. (32) yields

$$p_r^{(0)}(r,z) = p_0 r_1 \mathrm{e}^{-ik_{p0}(2z_1-z)} \sum_{n=1}^{N} \frac{A_n}{f_{rn}^{(0)}(z)} \mathrm{e}^{\frac{-B_n}{f_{rn}^{(0)}(z)}\left(\frac{r}{a}\right)^2} \tag{33}$$

with

$$f_{rn}^{(0)}(z) = 1 - i\frac{2z_1 - z}{z_n}. \tag{34}$$

The transmitted field $p_p^{(I0)}$ at $z = z_1$ is

$$p_p^{(I0)}(r,z) = \int_0^{+\infty} t_1 p_{ig}(r',z_1) g_p(r,z|r',z_1) r'\,\mathrm{d}r', \tag{35}$$

then

$$p_p^{(I0)}(r,z) = p_0 t_1 \mathrm{e}^{-ik_{p0}z_1} \mathrm{e}^{-ik_{p1}(z-z_1)} \cdot \sum_{n=1}^{N} \frac{A_n}{f_{pn}^{(I0)}(z)} \mathrm{e}^{\frac{-B_n}{f_{pn}^{(I0)}(z)}\left(\frac{r}{a}\right)^2} \tag{36}$$

with

$$f_{pn}^{(I0)}(z) = 1 - i\frac{z_1}{z_n} - i\eta\frac{z - z_1}{z_n} \tag{37}$$

and

$$\eta = \frac{k_0}{k_1}. \tag{38}$$

The reflected field $p_p^{(II0)}$ at $z = z_2$ is

$$p_p^{(II0)}(r,z) = \int_0^{+\infty} r_2 p_p^{(I0)}(r',z_2) g_p(r,z|r',z_2) r'\,\mathrm{d}r', \tag{39}$$

then

$$p_p^{(II0)}(r,z) = p_0 t_1 r_2 \mathrm{e}^{-ik_{p0}z_1} \mathrm{e}^{-ik_{p1}(z_2-z+d)} \cdot \sum_{n=1}^{N} \frac{A_n}{f_{pn}^{(II0)}(z)} \mathrm{e}^{\frac{-B_n}{f_{pn}^{(II0)}(z)}\left(\frac{r}{a}\right)^2} \tag{40}$$

with

$$f_{pn}^{(II0)}(z) = 1 - i\frac{z_1}{z_n} - i\eta\frac{z_2 - z + d}{z_n}. \tag{41}$$

The field $p_r^{(1)}$ is

$$p_r^{(1)}(r,z) = \int_0^{+\infty} t_2 p_p^{(II0)}(r',z_1) g_0(r,z|r',z_1) r'\,\mathrm{d}r', \tag{42}$$

then

$$p_r^{(1)}(r,z) = p_0 t_1 t_2 r_2 \mathrm{e}^{-ik_{p0}(2z_1-z)} \mathrm{e}^{-ik_{p1}2d} \cdot \sum_{n=1}^{N} \frac{A_n}{f_{rn}^{(1)}(z)} \mathrm{e}^{\frac{-B_n}{f_{rn}^{(1)}(z)}\left(\frac{r}{a}\right)^2} \tag{43}$$

with

$$f_{rn}^{(1)}(z) = 1 - i\frac{2z_1 - z}{z_n} - i\eta\frac{2d}{z_n}. \tag{44}$$

The reflected field $p_p^{(I1)}$at the interface $z = z_1$ is

$$p_p^{(I1)}(r,z) = \int_0^{+\infty} r_2 p_p^{(II0)}(r',z_1) g_p(r,z|r',z_1)\, r'\,\mathrm{d}r', \tag{45}$$

$$p_p^{(I1)}(r,z) = p_0 t_1 r_2^2 \mathrm{e}^{-ik_{p0}z_1} \mathrm{e}^{-ik_{p1}(z-z_1+2d)} \cdot \sum_{n=1}^{N} \frac{A_n}{f_{pn}^{(I1)}(z)} \mathrm{e}^{\frac{-B_n}{f_{pn}^{(I1)}(z)}\left(\frac{r}{a}\right)^2} \tag{46}$$

with

$$f_{pn}^{(I1)}(z) = 1 - i\frac{z_1}{z_n} - i\eta\frac{z - z_1 + 2d}{z_n}. \tag{47}$$

The reflected field $p_p^{(II1)}$ at $z = z_2$ is

$$p_p^{(II1)}(r,z) = \int_0^{+\infty} r_2 p_p^{(I1)}(r',z_2) g_p(r,z|r',z_2)\, r'\,\mathrm{d}r', \tag{48}$$

$$p_p^{(II1)}(r,z) = p_0 t_1 r_2^3 \mathrm{e}^{-ik_{p0}z_1} \mathrm{e}^{-ik_{p1}(z_2-z+3d)} \cdot \sum_{n=1}^{N} \frac{A_n}{f_{pn}^{(II1)}(z)} \mathrm{e}^{\frac{-B_n}{f_{pn}^{(II1)}(z)}\left(\frac{r}{a}\right)^2} \tag{49}$$

with

$$f_{pn}^{(II1)}(z) = 1 - i\frac{z_1}{z_n} - i\eta\frac{z_2 - z + 3d}{z_n}. \tag{50}$$

Finally, the field $p_r^{(2)}$ is

$$p_r^{(2)}(r,z) = \int_0^{+\infty} t_2 p_p^{(II1)}(r',z_1) g_0(r,z|r',z_1)\, r'\,\mathrm{d}r', \tag{51}$$

then

$$p_r^{(2)}(r,z) = p_0 t_1 t_2 r_2^3 \mathrm{e}^{-ik_{p0}(2z_1-z)} \mathrm{e}^{-ik_{p1}4d} \cdot \sum_{n=1}^{N} \frac{A_n}{f_{rn}^{(2)}(z)} \mathrm{e}^{\frac{-B_n}{f_{rn}^{(2)}(z)}\left(\frac{r}{a}\right)^2} \tag{52}$$

with

$$f_{rn}^{(2)}(z) = 1 - i\frac{2z_1 - z}{z_n} - i\eta\frac{4d}{z_n}. \tag{53}$$

The field $p_r^{(m)}$, for $m > 0$, can be written in the general form as

$$p_r^{(m)}(r,z) = p_0 t_1 t_2 r_2^{2m-1} \mathrm{e}^{-ik_{p0}(2z_1-z)} \mathrm{e}^{-ik_{p1}2md} \cdot \sum_{n=1}^{N} \frac{A_n}{f_{rn}^{(m)}(z)} \mathrm{e}^{\frac{-B_n}{f_{rn}^{(m)}(z)}\left(\frac{r}{a}\right)^2} \tag{54}$$

with

$$f_{rn}^{(m)}(z) = 1 - i\frac{2z_1 - z}{z_n} - i\eta\frac{2md}{z_n}. \tag{55}$$

The total reflected field is the sum of all reflected components

$$\begin{aligned} p_{rg}(r,z) &= \sum_{m=0}^{\infty} p_r^{(m)}(r,z) \\ &= p_0\,\mathrm{e}^{-ik_{p0}(2z_1-z)}\left(r_1\sum_{n=1}^{N}\frac{A_n}{f_{rn}^{(0)}(z)}\mathrm{e}^{\frac{-B_n}{f_{rn}^{(0)}(z)}\left(\frac{r}{a}\right)^2}\right. \\ &\quad + t_1 t_2\sum_{m=1}^{\infty} r_2^{2m-1}\mathrm{e}^{-ik_{p1}2md} \\ &\quad \left.\cdot\sum_{n=1}^{N}\frac{A_n}{f_{rn}^{(m)}(z)}\mathrm{e}^{\frac{-B_n}{f_{rn}^{(m)}(z)}\left(\frac{r}{a}\right)^2}\right). \end{aligned} \tag{56}$$

Putting

$$U_m = r_2^{2m-1}e^{-ik_{p1}2md}, \tag{57}$$

then

$$\begin{aligned} p_{rg}(r,z) = p_0\,\mathrm{e}^{-ik_{p0}(2z_1-z)}&\left(r_1\sum_{n=1}^{N}\frac{A_n}{f_{rn}^{(0)}(z)}\mathrm{e}^{\frac{-B_n}{f_{rn}^{(0)}(z)}\left(\frac{r}{a}\right)^2}\right. \\ &\left. + t_1 t_2\sum_{m=1}^{\infty}U_m\sum_{n=1}^{N}\frac{A_n}{f_{rn}^{(m)}(z)}\mathrm{e}^{\frac{-B_n}{f_{rn}^{(m)}(z)}\left(\frac{r}{a}\right)^2}\right). \end{aligned} \tag{58}$$

3.3. Transmitted field

The transmitted field $p_t^{(0)}$ at $z = z_2$ is

$$p_t^{(0)}(r,z) = \int_0^{+\infty} t_2 p_p^{(I0)}(r',z_2)g_0(r,z|r',z_2)r'\,\mathrm{d}r', \tag{59}$$

which gives

$$\begin{aligned} p_t^{(0)}(r,z) &= p_0\,t_1\,t_2\mathrm{e}^{-ik_{p0}(z-d)}\mathrm{e}^{-ik_{p1}d} \\ &\quad\cdot\sum_{n=1}^{N}\frac{A_n}{f_{tn}^{(0)}(z)}\mathrm{e}^{\frac{-B_n}{f_{tn}^{(0)}(z)}\left(\frac{r}{a}\right)^2} \end{aligned} \tag{60}$$

with

$$f_{tn}^{(0)}(z) = 1 - i\frac{z-d}{z_n} - i\eta\frac{d}{z_n}, \tag{61}$$

and the transmitted field $p_t^{(1)}$ at $z = z_2$ is

$$p_t^{(1)}(r,z) = \int_0^{+\infty} t_2 p_p^{(I1)}(r',z_2)g_0(r,z|r',z_2)r'\,\mathrm{d}r', \tag{62}$$

then

$$\begin{aligned} p_t^{(1)}(r,z) &= p_0\,t_1\,t_2 r_2^2\mathrm{e}^{-ik_{p0}(z-d)}\mathrm{e}^{-ik_{p1}3d} \\ &\quad\cdot\sum_{n=1}^{N}\frac{A_n}{f_{tn}^{(1)}(z)}\mathrm{e}^{\frac{-B_n}{f_{tn}^{(1)}(z)}\left(\frac{r}{a}\right)^2} \end{aligned} \tag{63}$$

with

$$f_{tn}^{(1)}(z) = 1 - i\frac{z-d}{z_n} - i\eta\frac{3d}{z_n}. \tag{64}$$

In the same manner

$$\begin{aligned} p_t^{(m)}(r,z) &= p_0\,t_1\,t_2 r_2^{2m}\mathrm{e}^{-ik_{p0}(z-d)}\mathrm{e}^{-ik_{p1}(2m+1)d} \\ &\quad\cdot\sum_{n=1}^{N}\frac{A_n}{f_{tn}^{(m)}(z)}\mathrm{e}^{\frac{-B_n}{f_{tn}^{(m)}(z)}\left(\frac{r}{a}\right)^2} \end{aligned} \tag{65}$$

with

$$f_{tn}^{(m)}(z) = 1 - i\frac{z-d}{z_n} - i\eta\frac{(2m+1)d}{z_n}. \tag{66}$$

Putting

$$V_m = r_2^{2m}\mathrm{e}^{-ik_{p1}(2m-1)d}, \tag{67}$$

the total transmitted field is

$$\begin{aligned} p_{tg}(r,z) &= \sum_{m=0}^{\infty} p_t^{(m)}(r,z) = p_0\,t_1\,t_2\,\mathrm{e}^{-ik_{p0}(z-d)} \\ &\quad\cdot\sum_{m=0}^{\infty}V_m\sum_{n=1}^{N}\frac{A_n}{f_{tn}^{(m)}(z)}\mathrm{e}^{\frac{-B_n}{f_{tn}^{(m)}(z)}\left(\frac{r}{a}\right)^2}. \end{aligned} \tag{68}$$

3.4. Field inside the plate

According to Fig. 1, the field inside the plate is

$$\begin{aligned} p_{pg}(r,z) &= p_p^{(I0)} + p_p^{(II0)} + p_p^{(I1)} + p_p^{(II1)} \\ &\quad + p_p^{(I2)} + p_p^{(II2)} + \ldots \end{aligned} \tag{69}$$

The field $p_p^{(Im)}$ can be generalized as follows

$$\begin{aligned} p_p^{(Im)}(r,z) &= p_0\,t_1\,r_2^{2m}\mathrm{e}^{-ik_{p0}z_1}\mathrm{e}^{-ik_{p1}(z-z_1+2md)} \\ &\quad\cdot\sum_{n=1}^{N}\frac{A_n}{f_{pn}^{(Im)}(z)}\mathrm{e}^{\frac{-B_n}{f_{pn}^{(Im)}(z)}\left(\frac{r}{a}\right)^2} \end{aligned} \tag{70}$$

with

$$f_{pn}^{(Im)}(z) = 1 - i\frac{z_1}{z_n} - i\eta\frac{z - z_1 + 2md}{z_n}. \tag{71}$$

Putting

$$W_m = r_2^{2m}\mathrm{e}^{-ik_{p1}2md}, \tag{72}$$

then

$$\begin{aligned} p_p^{(Im)}(r,z) &= p_0\,t_1\mathrm{e}^{-ik_{p0}\,z_1}\mathrm{e}^{-ik_{p1}(z-z_1)}W_m \\ &\quad\cdot\sum_{n=1}^{N}\frac{A_n}{f_{pn}^{(Im)}(z)}\mathrm{e}^{\frac{-B_n}{f_{pn}^{(Im)}(z)}\left(\frac{r}{a}\right)^2}. \end{aligned} \tag{73}$$

The field $p_p^{(IIm)}$ can be generalized as follows

$$\begin{aligned} p_p^{(IIm)}(r,z) &= p_0\,t_1\,r_2^{2m+1}\mathrm{e}^{-ik_{p0}\,z_1} \\ &\quad\cdot\mathrm{e}^{-ik_{p1}(z_2-z+(2m+1)d)} \\ &\quad\cdot\sum_{n=1}^{N}\frac{A_n}{f_{pn}^{(IIm)}(z)}\mathrm{e}^{\frac{-B_n}{f_{pn}^{(IIm)}(z)}\left(\frac{r}{a}\right)^2}, \end{aligned} \tag{74}$$

then

$$p_p^{(IIm)}(r,z) = p_0\, t_1\, r_2 \mathrm{e}^{-ik_{p0}\, z_1} \mathrm{e}^{-ik_{p1}(z_2-z+d)} W_m \cdot \sum_{n=1}^{N} \frac{A_n}{f_{pn}^{(IIm)}(z)} \mathrm{e}^{\frac{-B_n}{f_{pn}^{(IIm)}(z)}\left(\frac{r}{a}\right)^2} \tag{75}$$

with

$$f_{pn}^{(IIm)}(z) = 1 - i\frac{z_1}{z_n} - i\eta\frac{z_2 - z + (2m+1)d}{z_n}. \tag{76}$$

The total fields are expressed

$$\begin{aligned} p_p^I(r,z) &= \sum_j p_p^{(Im)}(r,z) \\ &= p_0\, t_1 \mathrm{e}^{-ik_{p0}\, z_1} \mathrm{e}^{-ik_{p1}(z-z_1)} \cdot \sum_m W_m \sum_{n=1}^{N} \frac{A_n}{f_{pn}^{(Im)}(z)} \mathrm{e}^{\frac{-B_n}{f_{pn}^{(Im)}(z)}\left(\frac{r}{a}\right)^2}, \end{aligned} \tag{77}$$

$$\begin{aligned} p_p^{II}(r,z) &= \sum_j p_p^{(IIm)}(r,z) \\ &= p_0\, t_1\, r_2 \mathrm{e}^{-ik_{p0}\, z_1} \mathrm{e}^{-ik_{p1}(z_2-z+d)} \cdot \sum_m W_m \sum_{n=1}^{N} \frac{A_n}{f_{pn}^{(IIm)}(z)} \mathrm{e}^{\frac{-B_n}{f_{pn}^{(IIm)}(z)}\left(\frac{r}{a}\right)^2}. \end{aligned} \tag{78}$$

The field inside the plate is then

$$p_{pg}(r,z) = p_p^I(r,z) + p_p^{II}(r,z). \tag{79}$$

3.5. Green's function for an immersed plate

From Eq. (68) the transmitted field is expressed as

$$p_{tg}(r,z) = t_1\, t_2 \int_0^{+\infty} p_{ig}(r',z_1) g(r,z|r',z_2) r'\, \mathrm{d}r' \tag{80}$$

with

$$g(r,z|r',z_2) = \sum_{m=0}^{\infty} H_m g_m(r,z|r',z_2), \tag{81}$$

$$g_m(r,z|r',z_2) = \frac{ik}{2(z-z_m)} J_0\left(\frac{k_{p0} r r'}{z-z_m}\right) \mathrm{e}^{-ik_{p1}\frac{r^2+r'^2}{2(z-z_m)}}, \tag{82}$$

$$z_m = z_2 + \eta(2m+1)d, \tag{83}$$

$$H_m = V_m \mathrm{e}^{-ik_{p0}[z_1-(2m+1)d]}. \tag{84}$$

4. Results and discussions

The parameters used in simulation are a = 5 mm, f_0 = 2 MHz and p_0 = 1.72 Pa.

Two types of plates are studied, the first is made of plexiglas, the second is made of steel.

The acoustical parameters of the materials used in this study are listed in Table 1 (Kinsler *et al.*, 1999).

Table 1. Acoustical parameters of used material at 2 MHz.

Medium	Water	Plexiglas	Steel
Density ρ [kg/m^3]	998	1200	7700
Longitudinal velocity c_l [m/s]	1481	2650	6100
Attenuation coefficient α [Np*/m]	0	46	10
Wavelength λ [10^{-3} m]	0.741	1.325	3.05
Wave number k [rad/m]	8485	4742	2060

*Np: Neper $\left(1\ \mathrm{Np} = \frac{20}{\ln(10)}\ \mathrm{dB} \approx 8.69\ \mathrm{dB}\right)$.

4.1. Validation of the model

The results obtained based on the Gaussian beams decomposition were compared to those provided by the angular spectrum method.

Figure 2 shows the axial distributions of pressure in the case of a plexiglas plate 3 mm thick.

Noting that: z_1 = 32.26 mm, z_2 = 35.26 mm, z_f = 33.76 mm and $2z_f$ = 67.52 mm.

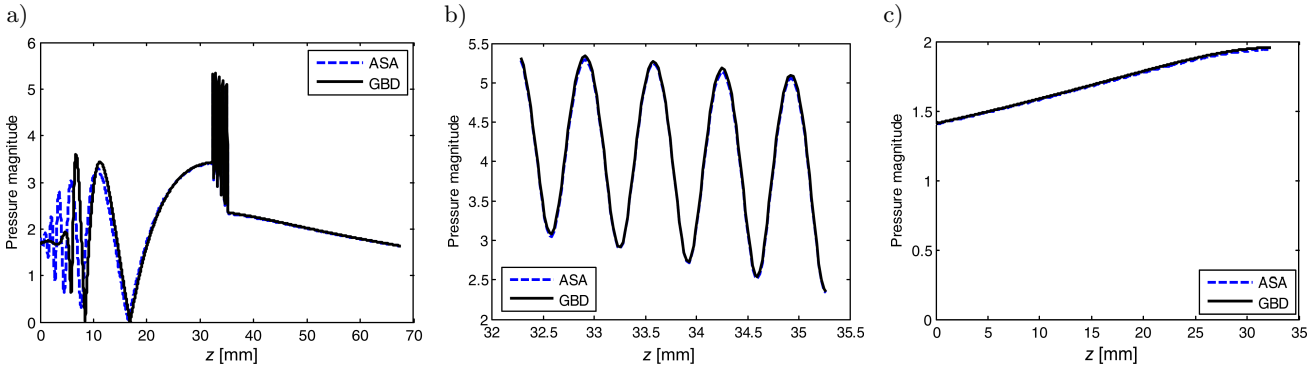

Fig. 2. Axial distributions of pressure (a), inside the plate (b), and reflected (c) (solid curve: GBD, dashed curve: ASA) for plexiglas plate.

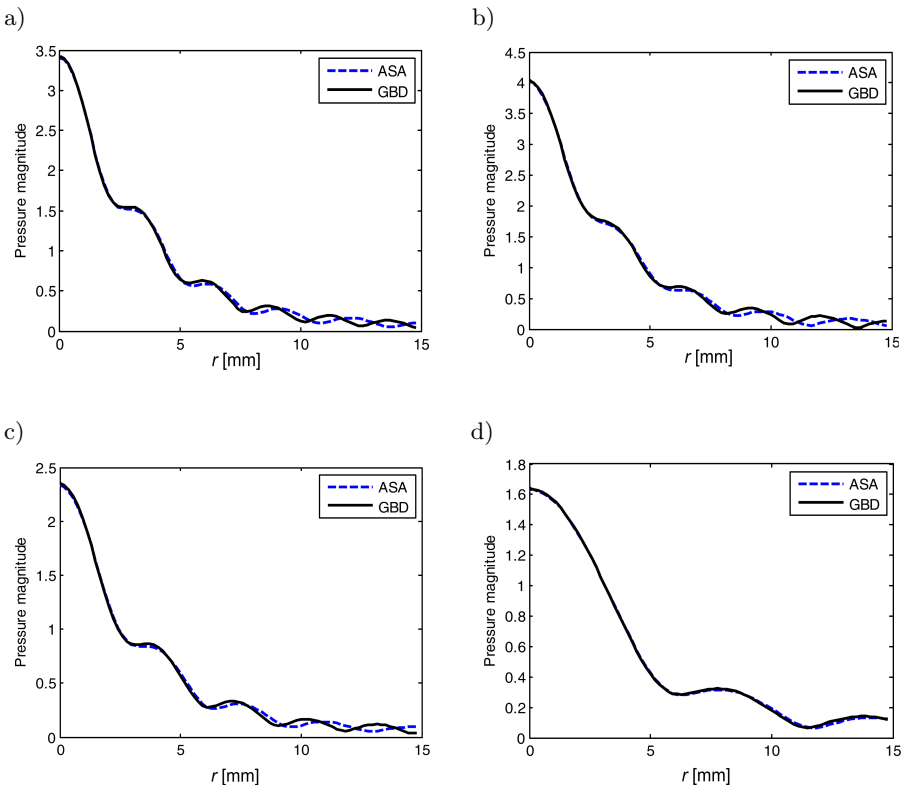

Fig. 3. Radial distributions of pressure. Incident field at z_1 (a), internal field at z_f (b), and transmitted field at z_2 (c) and at $2z_f$ (d) (solid curve: GBD, dashed curve: ASA) for plexiglas plate.

Figure 2b gives a zoom of the pressure distribution inside the plate. There is a periodicity of $l = 670$ µm which corresponds to the half wavelength in the plexiglas. These oscillations are due to resonance of the acoustic field inside the plate. The reflected field is presented in Fig. 2c. The two techniques show a good agreement, unless in the region of the very near field (Fig. 2a). The discrepancy is due to the fact that GBD doesn't take into account the vanishing mode. It can also be explained by the limited number of A_n and B_n coefficients (Eq. (26)).

Figure 3 shows the radial distributions of pressure, of the incident field at $z = z_1$ (Fig. 3a), of the internal field at $z = z_f$ (Fig. 3b), and of the transmitted field at $z = z_2$ (Fig. 3c) and at $z = 2z_f$ (Fig. 3d) in the case of a plexiglas plate 3 mm thick.

Examining curves, good similarity between results provided by the two models is observed. Consequently, the GBD technique offers a very simple modeling method comparing to the ASA technique.

4.2. Characterization of the plate

We define the reflection and transmission coefficients as

$$R = \frac{1}{p_0}\int_0^a 2\pi\, p_r(r,0) r\,\mathrm{d}r, \tag{85}$$

$$T = \frac{1}{p_0}\int_0^a 2\pi\, p_t(r,2z_f) r\,\mathrm{d}r. \tag{86}$$

Using Eq. (58), the reflection coefficient in the case of using the GBD technique is

$$R_g = \frac{1}{p_0}\int_0^a 2\pi\, p_{rg}(r,0) r\,\mathrm{d}r, \tag{87}$$

$$R_g = \int_0^a 2\pi\, \mathrm{e}^{-ik_{p0}(2z_1)}\left(r_1 \sum_{n=1}^{N} \frac{A_n}{f_{rn}^{(0)}(0)} \mathrm{e}^{\frac{-B_n}{f_{rn}^{(0)}(0)}\left(\frac{r}{a}\right)^2} + t_1 t_2 \sum_{m=1}^{\infty} U_m \sum_{n=1}^{N} \frac{A_n}{f_{rn}^{(m)}(0)} \mathrm{e}^{\frac{-B_n}{f_{rn}^{(m)}(0)}\left(\frac{r}{a}\right)^2}\right) r\,\mathrm{d}r, \tag{88}$$

then

$$R_g = \pi a^2\, \mathrm{e}^{-ik_{p0}(2z_1)}\left[r_1 \sum_{n=1}^{N} \frac{A_n}{B_n}\left(1 - \mathrm{e}^{\frac{-B_n}{f_{rn}^{(0)}(0)}}\right) + t_1 t_2 \sum_{m=1}^{\infty} U_m \sum_{n=1}^{N} \frac{A_n}{B_n}\left(1 - \mathrm{e}^{\frac{-B_n}{f_{rn}^{(m)}(0)}}\right)\right]. \tag{89}$$

Using Eq. (68), the transmission coefficient in the case of using the GBD technique is

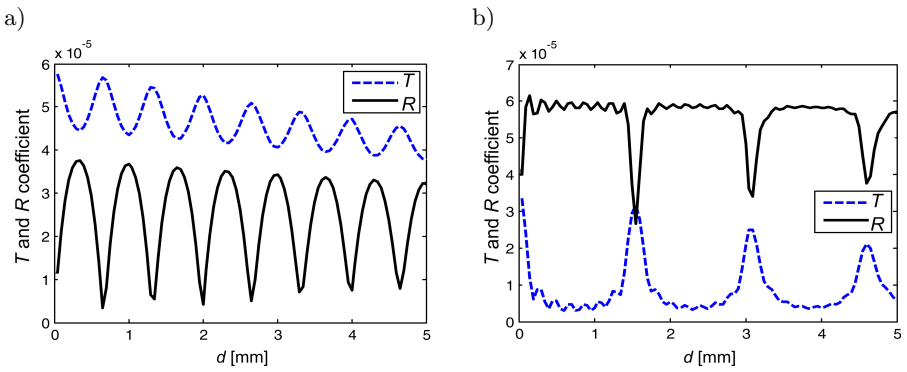

Fig. 4. Variations of the transmission coefficient T (dashed curve) and reflection coefficient R (solid curve) *versus* d, for plexiglas plate (a) and steel plate (b).

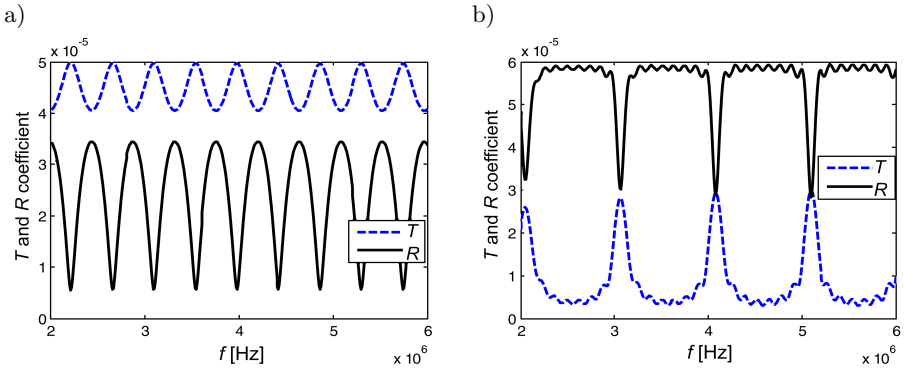

Fig. 5. Variations of the transmission coefficient T (dashed curve) and reflection coefficient R (solid curve) *versus* frequency f, for plexiglas plate (a) and steel plate (b).

$$T_g = \frac{1}{p_0}\int_0^a 2\pi\, p_{tg}(r, 2z_f)\, r\, \mathrm{d}r, \tag{90}$$

$$T_g = \int_0^a 2\pi\, t_1\, t_2\, \mathrm{e}^{-ik_{p0}(2z_f-d)} \sum_{m=0}^{\infty} V_m \cdot \sum_{n=1}^{N} \frac{A_n}{f_{tn}^{(m)}(2z_f)}\, \mathrm{e}^{\frac{-B_n}{f_{tn}^{(m)}(2z_f)}\left(\frac{r}{a}\right)^2} r\, \mathrm{d}r, \tag{91}$$

then

$$T_g = \pi a^2\, t_1\, t_2\, \mathrm{e}^{-ik_{p0}(2z_f-d)} \sum_{m=0}^{\infty} V_m \cdot \sum_{n=1}^{N} \frac{A_n}{B_n}\left(1 - \mathrm{e}^{\frac{-B_n}{f_{tn}^{(m)}(2z_f)}}\right). \tag{92}$$

Figure 4 shows changes of the reflection and the transmission coefficients calculated using the GBD technique versus the thickness d in the both cases of plexiglas and steel plate made.

We notice as expected that the resonance appears every $\frac{\lambda}{2}$. So $\Delta d_p = \frac{\lambda}{2} = \frac{c_p}{2f_0}$. $\Delta d_{Plx} = 0.67$ mm then $c_{Plx} \approx 2680$ m/s. $\Delta d_{St} = 1.525$ mm then $c_{St} \approx 6100$ m/s.

Figure 5 provides variations of the reflection and the transmission coefficients calculated with the GBD technique as a function of the frequency f. We observe that the difference in frequency between two successive resonances Δf corresponds to $\Delta f = \frac{c_p}{2d}$. Knowing one of the two parameters c_p or d, we can deduce the other. $\Delta f_{Plx} = 0.44$ MHz then $d_{Plx} \approx 3.01$ mm. $\Delta f_{St} = 1.01$ MHz then $d_{St} \approx 3.02$ mm.

As a conclusion, the derived technique helps characterizing materials of studied plates.

5. Conclusion

In this paper, a new analytical method for calculating the transmitted and the reflected fields by an immersed plate is presented. This method takes into account absorption and diffraction phenomena as well as the multiple reflections inside the plate. It is based on Gaussian beam decomposition of the generated pressure field. Besides, a Green's function is also proposed to make it easy to model the propagated field.

The proposed model permits simulating the different fields (incident, transmitted and reflected fields) upstream, inside and downstream the plate. We use it as well to analyze variations of transmission and reflection coefficients of the plate as a function of the

thickness of the plate and the frequency. This analysis allows physical characterization of the plate.

The validity of this model is proven by comparing the results obtained by the proposed model to those given by the Angular Spectrum Approach (ASA).

References

1. Aouzale N., Chitnalah A., Jakjoud H. (2010), *Moroccan oil characterization using pulse-echo ultrasonic technique*, Physical & Chemical News, **54**, 1–8.
2. Babich V. M., Pankratova T.F. (1973), *On discontinuities of the Green function of mixed problem for wave equation with variable coefficients*, Problems of Mathematical Physics, Leningrad University Press, **6**, 9–27.
3. Blitz J., Simpson G. (1996), *Ultrasonic methods of non-destructive testing*, Chapman & Hall, London.
4. Carcione J.M. (1996), *Wave propagation in anisotropic, saturated porous media: Plane-wave theory and numerical simulation*, The Journal of the Acoustical Society of America, **99**, 5, 2655–2666.
5. Cartz L. (1995), *Nondestructive testing*, ASM International, Materials Park, OH, United States.
6. Cerveny V., Popov M.M., Psencik I. (1982), *Computation of wave fields in inhomogeneous media – Gaussian beam approach*, Geophysical Journal of Royal Astronomical Society, **70**, 109–128.
7. Deschamps M., Hosten B. (1992), *The effects of viscoelasticity on the reflection and transmission of ultrasonic waves by an orthotropic plate*, The Journal of the Acoustical Society of America, **91**, 4, 2007–2015.
8. Du Y., Jensen H., Jensen J.A. (2009), *Angular spectrum simulation of pulsed ultrasound fields*, IEEE International Ultrasonics Symposium Proceedings, 2379–2382.
9. Du Y., Jensen H., Jensen J.A. (2013), *Investigation of an angular spectrum approach for pulsed ultrasound fields*, Ultrasonics, **53**, 6, 1185–1191.
10. El Mouhtadi A., Duclos J., Duflo H. (2012), *Ultrasonic modeling of a viscoelastic homogeneous plate*, Acoustics 2012 Proceedings, Société Française d'Acoustique, Nantes, France, 2611–2616.
11. Glauser A.R., Robertson P.A., Lowe C.R. (2001), *An electrokinetic sensor for studying immersed surfaces, using focused ultrasound*, Sensors and Actuators B: Chemical, **80**, 1, 68–82.
12. Goodman J.W. (1968), *Introduction to fourier optics*, McGraw-Hill, New York, USA.
13. Green G. (1852), *An essay on the application of mathematical analysis to the theories of electricity and magnetism*, Journal für die reine und angewandte Mathematik, **44**, 356–374.
14. Gunarathne G.P.P., Christidis K. (2002), *Material characterization in situ using ultrasound measurements*, IEEE Transactions on Instrumentation and Measurement, **51**, 2, 368–373.
15. Hamilton M.F., Blackstock D.T. (1998), *Nonlinear acoustics*, San Diego, Academic Press.
16. Hull J.B., Langton C.M., Barker S., Jones A.R. (1996), *Identification and characterization of materials by broadband ultrasonic attenuation analysis*, Journal of Materials Processing Technology, **56**, 148–157.
17. Ingard K.U., Morse P.M. (1968), *Theoretical acoustics*, Princeton University Press, Princeton, New Jersey.
18. Jakjoud H., Chitnalah A., Aouzale N. (2014), *Transducer profile effect on the second harmonic level*, Acoustical Physics, **60**, 3, 261–268.
19. Kachalov A.P., Popov M.M. (1981), *Application of the method of summation of Gaussian beams for calculation of high-frequency wave fields*, Soviet Physics – Doklady, **26**, 604–606.
20. Kinra V.K., Dayal V. (1988), *A new technique for ultrasonic-nondestructive evaluation of thin specimens*, Experimental Mechanics, **33**, 2, 288–297.
21. Kinra V.K., Iyer V.R. (1995), *Ultrasonic measurement of the thickness, phase velocity, density or attenuation of a thin-viscoelastic plate. Part I. The forward problem*, Ultrasonics, **33**, 2, 95–109.
22. Kinsler L.E., Frey A.R., Coppens A.B., Sanders J.V. (1999), *Fundamentals of acoustics*, 4th Edition, Wiley-VCH.
23. Kline R.A. (1984), *Measurement of attenuation and dispersion using an ultrasonic spectroscopy technique*, The Journal of the Acoustical Society of America, **76**, 2, 498–504.
24. Korenev B.G. (2002), *Bessel functions and their applications*, Taylor & Francis, CRC Press.
25. Langenberg K.J., Marklein R., Mayer K. (2012), *Ultrasonic nondestructive testing of materials: theoretical foundations*, Taylor & Francis, CRC Press.
26. Lee B.C., Staszewski W.J. (2003a), *Modelling of Lamb waves for damage detection in metallic structures. Part I. Wave propagation*, Smart Materials and Structures, **12**, 5, 804–814.
27. Lee B.C., Staszewski W.J. (2003b), *Modelling of Lamb waves for damage detection in metallic structures: Part II. Wave interactions with damage*, Smart Materials and Structures, **12**, 5, 815–824.
28. Lee B.C., Staszewski W.J. (2007a), *Lamb wave propagation modelling for damage detection. I. Two-dimensional analysis*, Smart Materials and Structures, **16**, 2, 249–259.
29. Lee B.C., Staszewski W.J. (2007b), *Lamb wave propagation modelling for damage detection. II. Damage monitoring strategy*, Smart materials and structures, **16**, 2, 260–274.
30. Leiderman R., Braga A.M.B., Barbone P.E. (2005), *Scattering of ultrasonic waves by defective adhesion interfaces in submerged laminated plates*, The Journal of the Acoustical Society of America, **118**, 4, 2154–2166.

31. Lowe M.J.S. (1995), *Matrix techniques for modeling ultrasonic waves in multilayered media*, IEEE Transactions on Ultrasonics, Ferroelectrics, and Frequency Control, **42**, 4, 525–542.
32. Makin I.R.S., Averkiou M.A., Hamilton M.F. (2000), *Second-harmonic generation in a sound beam reflected and transmitted at a curved interface*, The Journal of the Acoustical Society of America, **108**, 4, 1505–1513.
33. Moilanen P., Nicholson P.H.F., Kilappa V., Cheng S., Timonen J. (2006), *Measuring guided waves in long bones: Modeling and experiments in free and immersed plates*, Ultrasound in Medicine & Biology, **32**, 5, 709–719.
34. Orofino D.P., Pedersen P.C. (1993a), *Efficient angular spectrum decomposition of acoustic sources. Part I. Theory*, IEEE Transactions on Ultrasonics, Ferroelectrics, and Frequency Control, **40**, 3, 238–249.
35. Orofino D.P., Pedersen P.C. (1993b), *Efficient angular spectrum decomposition of acoustic sources. Part II. Results*, IEEE Transactions on Ultrasonics, Ferroelectrics, and Frequency Control, **40**, 3, 250–257.
36. Perdijon J. (1993), *Ultrasonic non-destructive testing* [in French: *Le contrôle non destructif par ultrasons*], Hermès.
37. Popov M.M. (1982a), *A new method of computation of wave fields using Gaussian beams*, Wave Motion, **4**, 85–97.
38. Popov M.M. (1982b), *A new method of computing wave fields in the high-frequency approximation*, Journal of Mathematical Sciences, **20**, 1869–1882.
39. Popov M.M., Psencik I., Cerveny V. (1980), *Uniform ray asymptotics for seismic wave fields in laterally inhomogeneous media*, Prog. Abstr. XVII General Assembly of the European Seismological Commission, Hungarian Geophysical Society, Budapest, 143.
40. Rose J.L. (1999), *Ultrasonic waves in solid media*, Cambridge University Press, Cambridge.
41. Rossi M. (1986), *Electro-acoustique*, Edit. Dunod.
42. Schmerr L.W., Jr. (2013), *Fundamentals of ultrasonic nondestructive evaluation: a modeling approach*, Springer Science & Business Media.
43. Seki H., Granato A., Truell R. (1956), *Diffraction effects in the ultrasonic field of a piston source and their importance in the accurate measurement of attenuation*, The Journal of the Acoustical Society of America, **28**, 2, 230–238.
44. Shankar P.M. (2001), *Ultrasonic tissue characterization using a generalized Nakagami model*, IEEE Transactions on Ultrasonics, Ferroelectrics, and Frequency Control, **48**, 6, 1716–1720.
45. Soucrati H., Chitnalah A., Jakjoud H., El Idrissi A. (2013), *Application of the wavelets transform to the determination of the geometrical characteristics of a plate by analysis of the diffused acoustic field*, Revue Méditerranéenne des Télécommunications, **3**, 2, 152–156.
46. Van Hemelrijck D., Anastassopoulos A. (1996), *Non destructive testing*, A.A. Balkema, Rotterdam, Netherlands.
47. Wen J.J., Breazeale M.A. (1988), *A diffraction beam field expressed as the superposition of Gaussian beams*, The Journal of the Acoustical Society of America, **83**, 5, 1752–1756.
48. Westervelt P.J. (1963),*Parametric acoustic array*, The Journal of the Acoustical Society of America, **35**, 4, 535–537.
49. Williams E.G., Maynard J.D. (1982), *Numerical evaluation of the Rayleigh integral for planar radiators using the FFT*, The Journal of the Acoustical Society of America, **72**, 6, 2020–2030.
50. Wu P., Kazys R., Stepinski T. (1996a), *Analysis of the numerically implemented angular spectrum approach based on the evaluation of two-dimensional acoustic fields. Part I. Errors due to the discrete Fourier transform and discretization*, The Journal of the Acoustical Society of America, **99**, 3, 1339–1348.
51. Wu P., Kazys R., Stepinski T. (1996b), *Analysis of the numerically implemented angular spectrum approach based on the evaluation of two-dimensional acoustic fields. Part II. Characteristics as a function of angular range*, The Journal of the Acoustical Society of America, **99**, 3, 1349–1359.
52. Wu P., Kazys R., Stepinski T. (1997), *Optimal selection of parameters for the angular spectrum approach to numerically evaluate acoustic fields*, The Journal of the Acoustical Society of America, **101**, 1, 125–134.